Bioorganic & Medicinal Chemistry 20 (2012) 6613–6620

Contents lists available at SciVerse ScienceDirect

Bioorganic & Medicinal Chemistry

journal homepage: www.elsevier.com/locate/bmc

4-Isoxazolyl-1,4-dihydropyridines exhibit binding at the multidrug-resistance transporter

Victoria Hulubei [a], Scott B. Meikrantz [a], David A. Quincy [a], Tina Houle [a], John I. McKenna [a], Mark E. Rogers [a], Scott Steiger [b], N. R. Natale [a,b,*]

[a] Department of Chemistry, University of Idaho, Moscow, ID 83844-2343, United States
[b] Department of Biomedical and Pharmaceutical Sciences, The University of Montana, Missoula, MT 59812, United States

ARTICLE INFO

Article history:
Received 7 August 2012
Revised 4 September 2012
Accepted 13 September 2012
Available online 25 September 2012

Dedicated to the memory of Professor Robert O. Hutchins, peerless mentor and good friend.

Keywords:
Isoxazole
Dihydropyridine
Multidrug transporter
Adjuvant
Lateral metalation

ABSTRACT

The 4-isoxazolyl-dihydropyridines (IDHPs) exhibit inhibition of the multidrug-resistance transporter (MDR-1), and exhibit an SAR distinct from their activity at voltage gated calcium channels (VGCC). Among the four most active IDHPs, three were branched at C-5 of the isoxazole, including the most active analog, **1k**.

The multidrug-resistance transporter (MDR-1, also known as P-glycoprotein, P-gp) is a member of the ATP-binding cassette (ABC) superfamily of efflux pumps.[1,2] Molecules which inhibit this efflux pump are of interest in overcoming multidrug-resistance, and intense efforts are in progress towards developing effective and selective theranostic agents.[3,4] Termed multidrug-resistance reversers (MDRRs), several agents have advanced to clinical trials, as an example Tariquidar (XR9576) is presently in several advanced clinical trials in combination with chemotherapeutic agents as an adjuvant against multidrug resistance in cancer.[5]

4-Aryl-1,4-dihydropyridines (DHPs) that bind the L-type voltage gated calcium channel (VGCC) have been in general medical practice for over three decades,[6] The DHP framework serves as a useful scaffold, and more recently DHPs have been recognized as useful ligands of MDR-1.[7–10] The information regarding the corresponding structure activity relationship (SAR) at VGCC verses MDR-1 is emerging, and several structural distinctions may eventually lead to practical selectivity. An early observation was that heterocyclic rings in the 4-aryl position of DHPs enhanced the reversal of multidrug resistance and inhibited photoaffinity labeling of P-gp.[7] Another interesting observation is that while the (+)-enantiomers of DHPs usually possess superior activity at the VGCC, this enantioselectivity of action is not observed at the MDR-1, with the VGCC distomer being equally effective at reversing drug resistance.[11]

Replacement of the 4-aryl group of the DHPs with the bioisosteric isoxazole results in robust calcium antagonists,[12–19] and we have studied the resulting SAR, conformational dynamics and structural properties of the 4-isoxazolyl-DHPs (IDHPs, Chart 1). Given the bioactivity and unique SAR observed for VGCC activity of IDHPs, we reasoned that they should interact with the MDR-1, based on the common pharmacophore model illustrated in Figure 1 of known MDR-1 ligands nicardipine[3] and dexniguldpine[10] with an IDHP **1** analog. Furthermore, it is plausible that chemistry developed in our laboratories for the functionalization of isoxazoles could be applied to developing IDHPs with selectivity for MDR-1 over the VGCC.

1. Chemistry

Known IDHPs were prepared as previously described.[12–19] The new IDHPs **1k** and **1l** were prepared from isoxazolyl-oxazoline **2** using our lateral metalation and electrophilic quenching methodology,[20,21] as outlined the Scheme 1 below. The isoxazoyl-oxazoline **2** was deprotonated using *n*-butyl lithium at low temperature, and

* Corresponding author.
E-mail address: Nicholas.natale@umontana.edu (N.R. Natale).

0968-0896/$ - see front matter © 2012 Elsevier Ltd. All rights reserved.
http://dx.doi.org/10.1016/j.bmc.2012.09.022

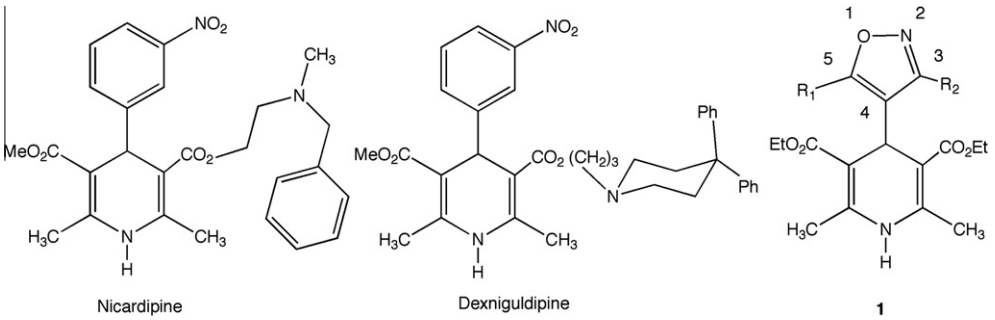

Chart 1. Nicardipine, dexniguldipine and isoxazolyl-dihydropyridines (IDHP) **1**, with numbering.

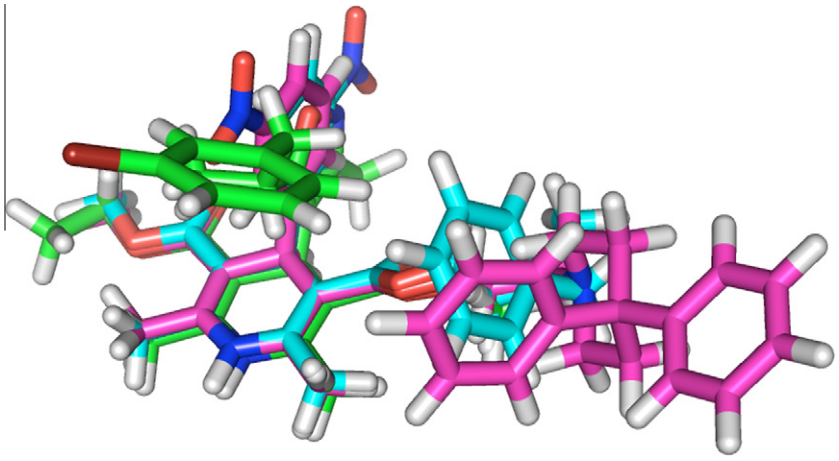

Figure 1. SYBYL common pharmacophore model of nicardipine (cyan), dexniguldipine (pink), and an analog of 4-Isoxazolyl-DHP **1k** (green).

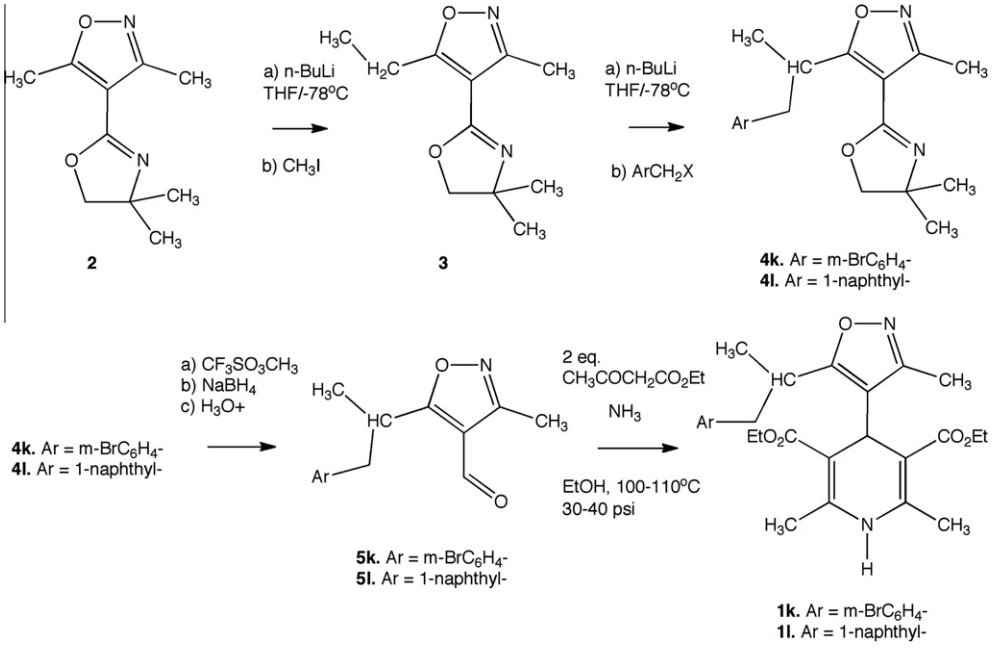

Scheme 1. Synthesis of branched IDHPs **1k** and **1l**.

electrophilic quenching provided 5-ethyl analog **3**, which was used to make both branched aryl analogs **1k** and **1l.** After the subsequent metalation and electrophilic quenching step, the oxazoline group was deprotected by methylation to the quaternary salt, reduction with sodium borohydride followed by mild aqueous hydrolysis to produce the corresponding aldehydes **5.** The Hantzsch procedure for branched aryl examples **1k** and **1l** required that the reaction be conducted at moderate pressure in an aerosol dispersion tube.

2. MDR-1 assay

Screening of IDHPs was performed by the Psychoactive Drug Screening Program (PDSP) of NIMH. The PDSP protocol utilizes live Caco-2 cells, which are derived from human colonic epithelium cells which express MDR-1.[22] The assay is based on the passive diffusion of calcein acetoxymethyl ester (Calcein-AM), which is hydrolyzed inside the cell to calcein, which is both fluorescent and negatively charged, and therefore trapped inside the cell. MDR-1 can transport non-fluorescent Calcein-AM from cells, but not hydrolzyed calcein. The assay measures the increase in calcein fluorescence as a function of time using a FlexStation II fluorimeter (Molecular Devices) in 96 well plates in which cells were preincubated with IDHPs (50 μM) for 30 min, upon which time calcein-AM was added to a final concentration of 150 nM. Fluorescence is monitored over 4 min, and each assay was performed in quadruplicate, with a 25 μM cyclosporin control. The value from untreated cells is 0% and the slope of the fluorescene is normalized taking the value for cyclosporin as 100%.[23]

In the event IDHPs exhibit robust MDR-1 activity in the PDSP protocol. An unsubstituted phenyl group at C-3 of the isoxazole provides MDR-1 inhibition (Table 1, Entry **1a**), however, both electron donating and withdrawing substituents appeared to lower biological activity (entries **1b** through **1f**). The C-5 aryl ethyl series proved to be more promising (entries **1h** to **1l**). The most potent VGCC IDHP in this series exhibited only slight MDR-1 activity, however branching at the C-5 position doubled its inhibition activity (entries **1j** vs **1l**). The branched bromophenyl analog **1k** provided the best activity in this series.

3. Conformational dynamics

One unique aspect of the DHPs is their conformational dynamics. Rotation around the isoxazole to DHP bond can give rise to either O-*exo* or O-*endo* conformers (Fig. 2) which — when the C-3 and/or C-5 substituent is large — gives rise to significantly diverse topologies. The barrier to this process is relatively low, on the order of 30–40 kJ mol^{-1}.[17]

Divergent conformations about the isoxazole to DHP bond have also been observed in crystallography, where, for example isoxazole C-5 methyl **1a** crystallized *O-endo*,[13] while its C-5 isopropyl analog **1g** was observed *O-exo*.[14] Both the C-5 naphthylethyl **1j**[18] and the branched 2-propylphenyl[16] analogs crystallized with the C-5 arylethyl group over the DHP ring (*O-endo*).

In our homology model for VGCC activity of the IDHPs we found that the opposite conformer of C-3 aryl isoxazoles than that found in the solid state (*O-exo* for **1b-d**), with the bulky group pointing away from the DHP ring (*O-endo*), gave the best explanation for

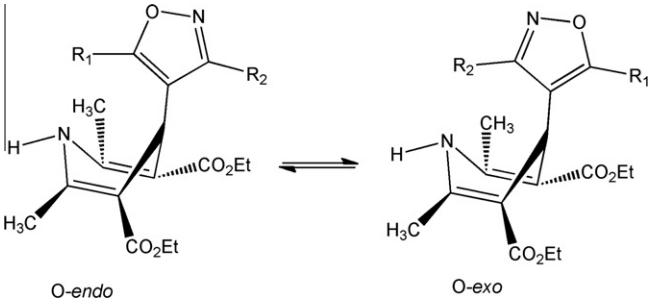

Figure 2. Rotation about the single bond between the heterocyclic rings gives rise to significant conformational differences.

VGCC activity of **1d-f** in our SAR.[19] Therefore, we usually find it necessary to consider conformational dynamics between the heterocyclic rings of IDHP in interpreting bioactivity.

4. Molecular modeling

The molecular models were constructed and visualized with INSIGHT 2000 on a Silicon Graphics Indigo II workstation. The rotational barrier calculations were performed using the torsion force constraint in the Discover module. The torsion was rotated through 360 intervals (1° increments) using a force constant of 10. After each rotation, the structure was subjected to 1000 steps of minimization, or until a rms value of 0.01 was reached, using the VA09A algorithm. The results of the conformational searches were examined with the Analysis module by constructing a graph of total energy vs. dihedral angle. The minimum and maximum energy calculated for conformations of **1k** are shown in Graph 1 and Graph 2, respectively.

The trend observed for the rotational barrier about the heterocyclic rings for the three molecules is **1l** > **1k** > **1d** (Table 2). The studies on **1d** have been published, along with VT-NMR studies which indicated the solution barrier was at or below the value calculated for rotation b.[19]

5. Solution spectra and nuclear Overhauser

Important structural features of the 4-aryl-DHPs are also maintained among IDHPs. Similar to 4-aryl rings of the most active 4-aryl-DHPs at the VGCC, the isoxazole ring is electron deficient. Comparable degrees of DHP ring pucker exist for both classes. The isoxazole ring similarly bisects that of the DHP ring, as shown in solid-state crystal structures, adopting either the O-*endo* or O-*exo* conformation in previous studies with the solid state preference for conformation at the heterocyclic ring juncture dictated by crystal packing forces rather than intrinsic energy differences.

Table 1
IDHP activity at VGCC and MDR-1

IDHP	R_1	R_2	VGCC K_i (nM)	VGCC Patch Clamp (μM)	Ref.	MDR-1 (% inh.)
1a	CH_3	C_6H_5	13.9		12,13,15	48.9
1b	CH_3	o-MeO-C_6H_4		17.1	19	32.8
1c	CH_3	2-MeO-5-Cl- C_6H_3		6.86	19	15.0
1d	CH_3	o-Cl-C_6H_4		9.68	19	10.9
1e	CH_3	m-Cl-C_6H_4		1.98	19	26.8
1f	CH_3	p-Cl-C_6H_4		1.31	19	11.7
1g	*i*-Pr	C_6H_5	[a]		14	38.4
1h	$C_6H_5CH_2CH_2$	C_6H_5	55.3		18	27.6
1i	p-Biphenyl-CH_2CH_2	CH_3	8.69		18	18.6
1j	1-Naphthyl CH_2CH_2	CH_3	4.1	0.47	18,19	19.0
1k	m-Br-$C_6H_5CH_2$ (CH_3)CH	CH_3			This work	61.2
1l	1-Naphthyl CH_2(CH_3)CH	CH_3			This work	38.3

[a] Weak vasodilator in the Langendorff perfused heart assay.

Table 2
Calculated free energy barriers for IDHPs (kcal mol^{-1})

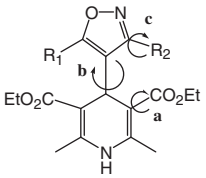

Rotation	1l	1k	1d
a	3.8	3.4	6.0
b	29.1	16.6	15.0
c	—	—	25.1

Gas phase calculations and solution studies both estimate a barrier to rotation below the energy available at physiological temperature. Thus, the conformation of the small molecule adapts to its macromolecular host.

This trend is confirmed in the room temperature ^{1}H NMR spectra for the new compound**s 1k** and **1l** at room temperature at 400 or 500 MHz. Two separate signals arise for the C-2 and C-6 methyl groups of the DHP for the naphthyl derivative **1l**, with a separation of 0.6 ppm (signals O and P, see Fig. 3). It is not possible to distinguish between the effects of diastereotopicity verses conformational constriction, although it seems likely that both exert an effect.

The calculations indicate lower energy for the O-*endo* conformation by about 17 kcal for **1l**. The 2D NOE experiment, on the other hand, shows the presence of both the O-*exo* and O-*endo* conformations, which indicates the actual barrier is at or below the calculated value.

NOE is observed for the DHP C-4 methine (I) and C-3′ isoxazole methyl protons (N), which reflects the *O-endo* conformation (Fig. 3). NOE between the same DHP C-4 methine (I) and the C-5′ α methine proton (M), in turn, evidences the *O-exo* conformation. This reveals that rotation about the heterocyclic ring junction, while not completely hindered, is restricted to the extent of causing a non-averaging of the two DHP methyl group protons.

Likewise, a similar, but lesser, effect is observed for the chiral 5-*m*Br-IDHP derivative **1k**. The room temperature ^{1}H NMR shows, again, a non-averaging of the signals for the C-2 and C-6 DHP methyl groups, with a separation this time of only 0.1 ppm (signals L and M, see Fig. 4). A similar pattern of nuclear Overhauser correlations again indicate the presence of both conformations at room temperature.

The common pharmacophore modelling studies of Ecker suggested a branched biaryl motif common to MDR-1 inhibitors.[24–26] A homology model based on the nucleotide binding site of MDR-1 by Reddy suggested a preferred inhibitory conformation wherein both 4-heteroaryl and C3 and C-5 aryl amides adopted a roughly *endo* relationship,[27] which is analogous to the pharmacophore model suggested by Eckert.[26] Based on consideration of the conformational dynamics of IDHPs, and available pharmacophore and homology modelling studies to date, we conclude that for optimal MDR-1 binding IDHPs likely adopt a conformation in which the branched aryl group is preferentially over the DHP moiety, or O-*endo* for **1k**, as illustrated in Figure 1. This leads us to conclude as a working hypothesis that a *conformational distinction may exist between VGCC and MDR-1 SAR for the activity of IDHPs*.

In summary, the IDHPs exhibit MDR-1 activity with an SAR that is distinct from VGCC activity, and provide an opportunity for further lead optimization. Our working hypothesis is that activity is optimal in the IDHP series for structures which have a branched

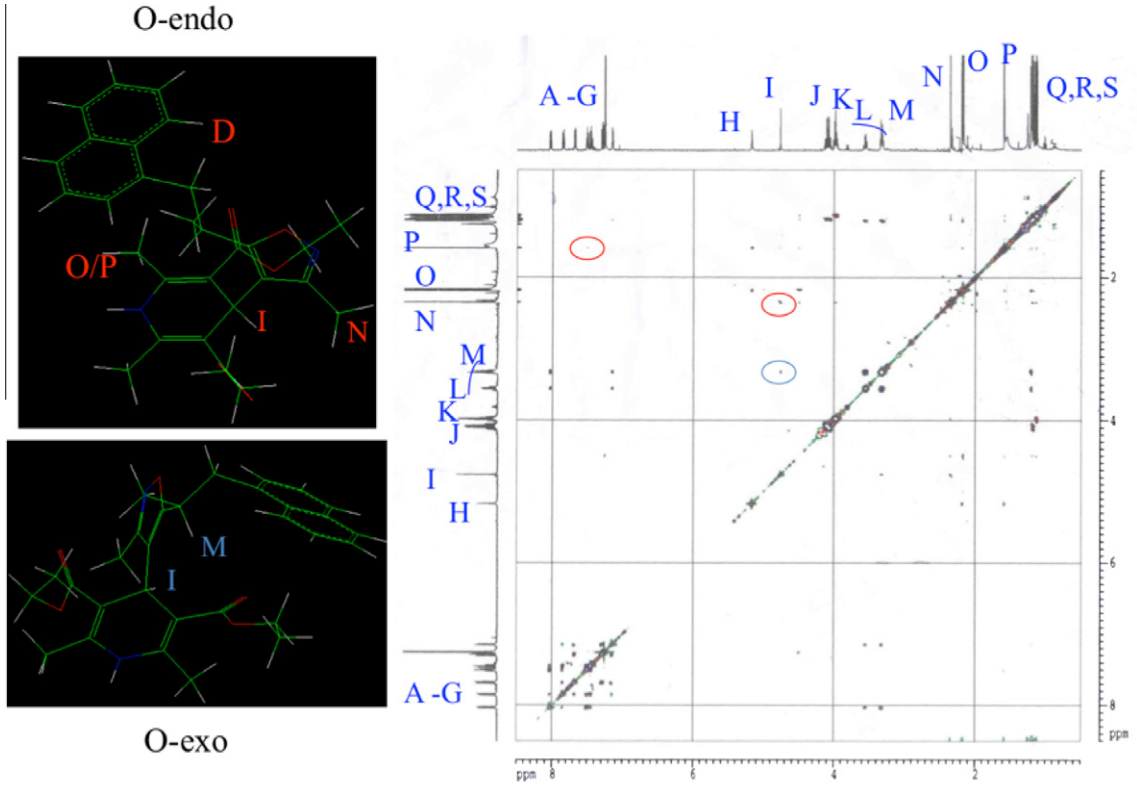

Figure 3. Nuclear Overhauser spectra of **1l.** The O-*endo* conformation is supported by the NOE signal between the DHP methyls at C-2 and C-6 (O,P) with the naphthyl aryl protons (D) and the DHP C-4 methina (I) and isoxzole C-3 methyl (N) (red circles). The DHP ring C-4 methine (I) and isoxazole C-5′ methine (M) correlation is evidence for the O-*exo* conformer (blue circle).

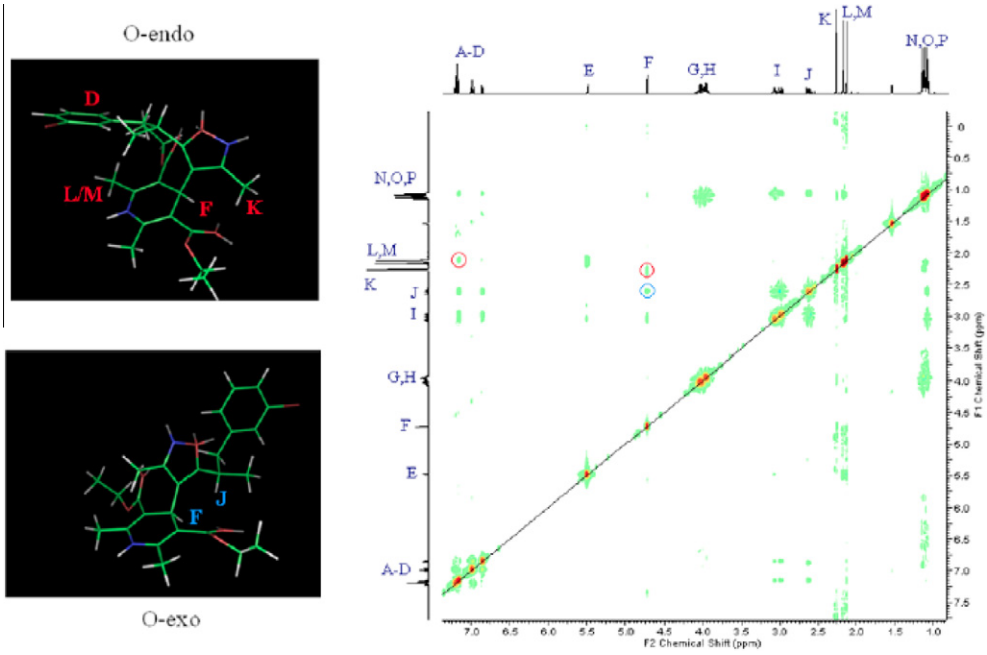

Figure 4. Nuclear Overhauser spectra of **1k**. The O-*endo* conformation is evidenced by the correlation between the aryl protons (A) and the 2,6-DHP methyls, (L,M) as well as by the C-3 isoxazole methyl group (K) with the DHP C-4 methine proton (F) (red circles). The DHP C-4 methine (F) correlation with the C-5 isoxazole methine (J) can only arise from the O-*exo* conformer (blue circle).

aryl–alkyl-heterocycle motif. Further analog synthesis and homology modeling studies are underway to test our working hypothesis, and will be reported in due course.

6. Experimental section

All chemicals were purchased from Aldrich Chemical Company and used without purification unless otherwise indicated. Solvents were reagent grade and dried just prior to use by standard methods. Melting points were determined in open capillary tubes on a Melt-Temp apparatus and are uncorrected. Radial chromatography was performed on a Harrison Associates chromatotron. Flash chromatography was performed using Baker Flash gel and in house compressed air. NMR spectra were recorded on a Bruker AC200 (200 MHz ^{1}H, 50 MHz ^{13}C), IBM Bruker AC300 (300 MHz ^{1}H, 75 MHz ^{13}C), or Avance Bruker DRX 500 (500 MHz ^{1}H, 125 MHz

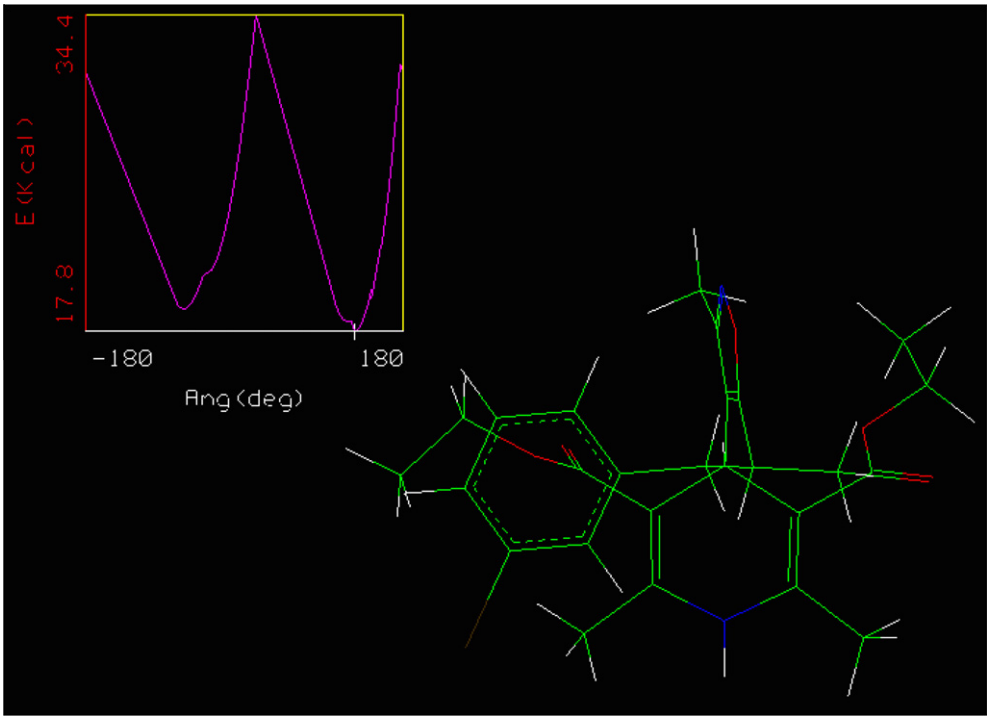

Graph 1. Low energy conformation for **1k** for rotation about the isoxazole-DHP bond. Marked as a white cross on the conformational analysis coordinates, upper left hand corner. The isoxazole is parallel to the hypothetical line from N-1 to C-4 of the DHP.

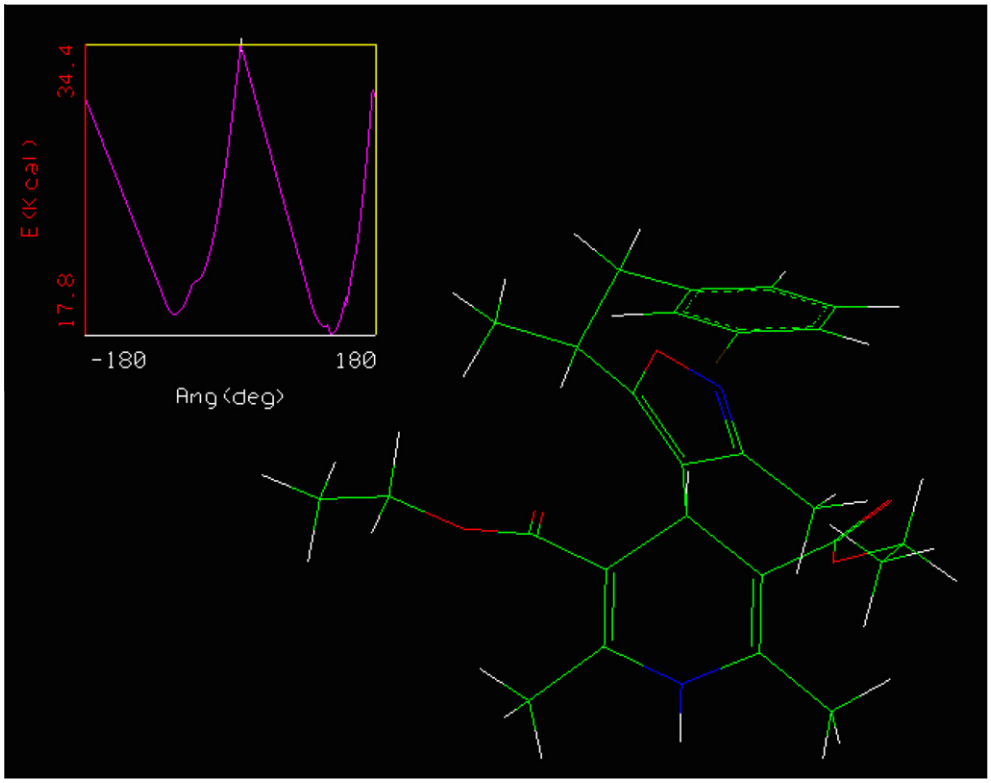

Graph 2. Saddle point maximum energy conformation for **1k** for rotation about the isoxazole-DHP bond. Marked as a white cross on the conformational analysis coordinates, upper left hand corner. The isoxazole is orthogonal to the hypothetical line from N-1 to C-4 of the DHP.

^{13}C) spectrometer, at ambient temperature in $CDCl_3$ unless otherwise specified. Chemical shifts are reported downfield from an internal tetramethylsilane (TMS) standard. Mass spectra were obtained on a JEOL AX 505-HA mass spectrometer using EI. Combustion analyses were performed by Desert Analytics, Tucson, AZ.

4-(4′,5′-Dihydro-4′,4′-dimethyl-Δ^2-oxazolin-2-yl)-3,5-dimethylisoxazole, (**2**), was prepared as previously described.[20]

6.1. Preparation of 5-ethyl, 3-methyl isoxazole oxazoline (3)

A dry 250-mL round-bottom flask was charged with isoxazolyloxazoline (**2**) (1.92 g, 9.88 mmol) and THF (100 mL) and cooled to −78 °C under N_2. A solution of *n*-BuLi in hexane (2.15 M, 5.1 mL, 10.9 mmol) was added via syringe dropwise. The yellow solution was stirred at −78 °C for 2 h, after which iodomethane (0.7 mL, 11.66 mmol) was added. The reaction was allowed to warm to room temperature overnight, and the solvent removed under vacuum to give a brown oil. The crude product was chromatographed on silica gel ($CHCl_3$) and Kugelrohr distilled (0.6 mm Hg, 67–73 °C) to give 1.95 g of **3** as a yellow oil (95%).

6.2. Diethyl 2,6-dimethyl-4-[5-(*RS*-1′-1-naphthyl-prop-2′-yl)-3-methylisoxazol-4-yl]-1,4-dihydropyridine-3,5-dicarboxylate (1l)

To a stirred solution of ethyl isoxazolyl oxazoline (**3**) from above (1.94 g, 9.30 mmol) in 100 mL dry THF cooled to −78 °C under N_2 was added 1.05 equiv of 2.15 M *n*-BuLi (4.5 mL) dropwise. The yellow solution was stirred at −78 °C for 2 h. Then 1-(chloromethyl)naphthalene, that had been just purified on a column of basic aluminum oxide, (1.5 mL, 10.0 mmol) was added dropwise and the reaction allowed to come to room temperature overnight. The mixture was concentrated under vacuum to give a brown oil which was purified by flash chromatography (silica gel, 95% hexane, 5% ETOAc) to give branched isoxazolyl-oxazoline **4l** as an 2.72 g amber oil (85%): ^{1}H NMR (500 MHz, $CDCl_3$) δ 1.22 (d, 6H, oxazoline Me's) 1.36 (d, 3H, lateral isoxazole C-5′ Me) 2.41 (s, 3H, isoxazole C-3′ Me) 3.25-3.30 (q, 1H, diastereotopic CH) and 3.52–3.56 (q, 1H, diastereoptopic CH) 3.58 (d, 1H, oxazoline CH) and 3.81 (d, 1H, other oxazoline CH) 4.15–4.22 (m, 1H, lateral isoxazole C-5′ C*H*) 7.21 (d, 1H, Ar-H_G) 7.35–7.38 (t, 1H, Ar-H_F) 7.48–7.56 (m, 2H, Ar-H_E,H_D) 7.73 (d, 1H, Ar-H_C) 7.86 (d?, 1H, Ar-H_B) 8.24 (d, 1H, Ar-H_A); Correlation between carbons and protons in CH_n fragments were determined by ^{1}H–13C HMQC and HMBC. Correlations between J coupled protons were determined by ^{1}H–^{1}H COSY.

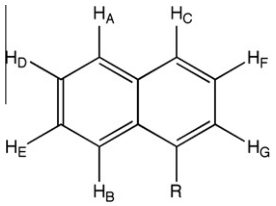

To a stirred solution of the product **4l** (3.60 g, 10.0 mmol) in 90 mL of dry CH_2Cl_2 was added 1.7 mL (2.45 g, 15.0 mmol) of distilled $CF_3SO_3CH_3$, and the mixture stirred under N_2 until TLC (silica, 80% hexane, 20% EtOAc) showed only baseline material. The mixture was cooled to 0 °C, and a solution of 0.69 g (18.2 mmol) of $NaBH_4$ in 25 mL of 4:1 THF/MeOH was added in one portion. This mixture was stirred at 0 °C for 30 min. Then 5 mL of saturated NH_4Cl was added and the mixture allowed to warm to room temperature. Ether, 50 mL, was added, and the layers were separated. The ether layer was washed with saturated NaCl (1 × 25 mL). The combined aqueous layers were extracted with CH_2Cl_2 (1 × 25 mL). The combined organic layers were dried over anhydrous Na_2SO_4, filtered, and concentrated to give an orange oil. The crude product was hydrolyzed with 15 mL of 1 M aqueous HCl in 20 mL of 4:1 THF/H_2O. The reaction mixture was poured into 50 mL of

ether, and the layers were separated. The ether layer was washed with saturated $NaHCO_3$ (3 × 25 mL). Combined aqueous layers were extracted with CH_2Cl_2 (1 × 25 mL) and the combined organic layers dried over anhydrous Na_2SO4, filtered, and concentrated to give the crude aldehyde as a yellow oil. The aldehyde was purified by flash chromatography (silica gel, 80% hexane, 15% EtOAc, 5% CH_2Cl_2) to give aldehyde **5l** as a pale-yellow oil which was used immediately in the next step: ^{1}H NMR (300 MHz, $CDCl_3$) δ 1.47 (d, 3H, lateral isoxazole C-5′ Me) 2.29 (s, 3H, isoxazole C-3′ Me) 3.39–3.42 (m, 2H, C*H*$_2$) 3.76–3.82 (m, 1H, C*H*) 7.01 (d, 1H, Ar-H) 7.20–7.29 (t, 1H, Ar-H) 7.42–7.47 (m, 2H, Ar-H) 7.67 (d, 1H, Ar-H) 7.78 (d, 1H, Ar-H) 7.86 (d, 1H, Ar-H) 9.17 (s, 1H, aldehyde H).

The aldehyde **5l** 0.37 g (1.33 mmol) was dissolved in ethanol (10 mL) and transferred to an aerosol dispersion tube to which ethyl acetoacetate (357 mg, 2.75 mmol) and aqueous ammonia (2 mL, 29.6%) were added. The mixture was heated to 100–110 °C for 48 h, the pressure rising to 30–40 psi. After cooling, the solvents were removed under vacuum to give a brown oil. The crude product was chromatographed on silica gel ($CHCl_3$) and purified by radial chromatography (40% hexane, 20% EtOAc, 10% CH_2Cl_2), giving 100 mg of **1l** as white crystals (15%): mp 144–146 °C; ^{1}H NMR (500 MHz, $CDCl_3$) δ 1.11–1.14 (t, 3H, C*H*$_3$CH$_2$O–) 1.17–1.19 (t, 3H, C*H*$_3$CH$_2$O–) 1.20 (d, 3H, lateral isoxazole C-5′ Me) 1.59 (s, 3H, DHP-Me) 2.18 (s, 3H, DHP-Me) 2.35 (s, 3H, isoxazole C-3′ Me) 3.30–3.35 (m, 2H, lateral isoxazole C-5′ C*H* and diastereotopic C*H*) 3.53–3.56 (m, 1H, other diastereotopic C*H*) 3.95–4.00 (m, 2H, CH$_3$C*H*$_2$O–) 4.05–4.13 (m, 2H, CH$_3$C*H*$_2$O–) 4.76 (s, 1H, DHP-C*H*) 5.25 (br s, 1H, N*H*) 7.15 (d, 1H, Ar-H$_G$) 7.27–7.30 (t, 1H, Ar-H$_F$) 7.43–7.52 (m, 2H, Ar-H$_E$, H$_D$) 7.68 (d, 1H, Ar-H$_C$) 7.85 (d, 1H, Ar-H$_B$) 8.03 (d, 1H, Ar-H$_A$); ^{13}C NMR (125 MHz, $CDCl_3$) δ 10.1 , 14.32, 14.38, 19.1, 19.5, 19.9, 28.9, 33.0, 37.0, 59.7, 59.8, 102.1, 102.4, 120.7, 123.5, 125.2, 125.4, 125.8, 126.8, 126.9, 128.9, 131.9, 134.0, 136.0, 142.3, 142.8, 159.8, 166.8, 167.3, 172.7; MS (EI) 502. Anal. Calcd for $C_{30}H_{34}N_2O_5$: C, 71.69; H, 6.82; N, 5.57. Found: C, 71.54; H, 6.63; N, 5.30.

6.3. Diethyl 2,6-dimethyl-4-[5-(*RS*-1′-*m*-bromophenyl-prop-2′-yl)-3-methylisoxazol-4-yl]-1,4-dihydropyridine-3,5-dicarboxylate (1k)

To a stirred solution of ethyl isoxazolyl-oxazoline (**3**) from above (2.69 g, 12.9 mmol) in 100 mL dry THF cooled to −78 °C under N_2 was added 1.1 equiv of 2.45 M *n*-BuLi (5.8 mL) dropwise. The yellow solution was stirred at −78 °C for 2 h. Then *m*-Br-benzylbromide (3.41 g, 13.7 mmol) dissolved in 10 mL dry THF was added dropwise and the reaction allowed to come to room temperature overnight. The mixture was concentrated under vacuum to give a brown oil which was purified by flash chromatography (silica gel, 80% hexane, 20% EtOAc) to give 4.30 g of branched isoxazolyl-oxazoline **4k** as a yellow oil (88%): ^{1}H NMR (200 MHz, $CDCl_3$) δ 1.27–1.31 (m, 9H, oxazoline Me's, lateral isoxazole C-5′ Me); 2.38 (s, 3H, isoxazole C-3′ Me) 2.69–2.80 (m, 1H, diastereotopic CH) and 2.96–3.06 (q, 1H, other diastereoptopic CH) 3.84–3.95 (m, 3H, oxazoline CH_2 and lateral isoxazole C-5′ C*H*) 6.97–7.11 (m, 2H, Ar-H) 7.26–7.34 (m, 1H, Ar-H); MS (EI) 376, 378.

To a stirred solution of the product **4k** (4.52 g, 12.0 mmol) in 100 mL of dry CH_2Cl_2 was added 2.0 mL (2.90 g, 17.7 mmol) of distilled $CF_3SO_3CH_3$, and the mixture stirred under N_2 until TLC (silica, 80% hexane, 20% EtOAc) showed only baseline material. The mixture was cooled to 0 °C, and a solution of 0.82 g (21.7 mmol) of $NaBH_4$ in 30 mL of 4:1 THF/MeOH was added in one portion. This mixture was stirred at 0 °C for 30 min. Then 7 mL of saturated NH_4Cl was added and the mixture allowed to warm to room temperature. Ether, 50 mL, was added, and the layers were separated. The ether layer was washed with saturated NaCl (1 × 25 mL). The combined aqueous layers were extracted with CH_2Cl_2 (1 × 25 mL). The combined organic layers were dried over anhydrous Na_2SO_4, filtered, and concentrated to give an orange oil. The crude product was hydrolyzed with 20 mL of 1 M aqueous HCl in 27 mL of 4:1 THF/H_2O. The reaction mixture was poured into 50 mL of ether, and the layers were separated. The ether layer was washed with saturated $NaHCO_3$ (3 × 25 mL). Combined aqueous layers were extracted with CH_2Cl_2 (1 x 25 mL) and the combined organic layers dried over anhydrous Na_2SO_4, filtered, and concentrated to give the crude aldehyde **5k** as a yellow oil. The aldehyde **5k** was purified by flash chromatography (silica gel, 80% hexane, 15% ETOAc, 5% CH_2Cl_2) to give 1.96 g as a pale-yellow oil (58 %): ^{1}H NMR (200 MHz, $CDCl_3$) δ 1.40 (d, 3H, lateral isoxazole C-5′ Me) 2.41 (s, 3H, isoxazole C-3′ Me) 2.85–3.07 (m, 2H, C*H*$_2$) 3.61–3.72 (q, 1H, C*H*) 6.97 (d, 1H, Ar-H) 7.06–7.13 (t, 1H, Ar-H) 7.22–7.33 (m, 1H, Ar-H) 9.66 (s, 1H, aldehyde H).

The aldehyde **5k** 1.96 g (6.36 mmol) was dissolved in ethanol (17 mL) and transferred to an aerosol dispersion tube to which ethyl acetoacetate (1.74 g, 13.3 mmol) and aqueous ammonia (1.5 mL, 29.6%) were added. The mixture was heated to 100–110 °C for 48 h, the pressure rising to 30–40 psi. After cooling, the solvents were removed under vacuum to give a brown oil. The crude product was chromatographed on silica gel (70% hexane, 30% ETOAc) and purified by radial chromatography (40% hexane, 20% EtOAc, 10% CH_2Cl_2), giving 600 mg of **1k** as white crystals (18%): mp 134–136 °C; ^{1}H NMR (500 MHz, $CDCl_3$) δ 1.13–1.21 (m, 9H, 2 C*H*$_3$CH$_2$O–, lateral isoxazole C-5′ Me) 2.19 (s, 3H, DHP-Me) 2.23 (s, 3H, DHP-Me) 2.33 (s, 3H isoxazole C-3′ Me) 2.67–2.72 (q, 1H, lateral isoxazole C-5′ C*H*) 3.03–3.16 (m, 2H, C*H*$_2$) 4.00–4.14 (m, 4H, 2 CH$_3$C*H*$_2$O–) 4.79 (s, 1H, DHP-C*H*) 5.48 (br s, 1H, N*H*) 6.92 (d, 1H, Ar-H) 7.04–7.07 (t, 1H, Ar-H) 7.24 (t, 1H, Ar-H) 7.27–7.30 (m, 1H, Ar-H); ^{13}C NMR (125 MHz, $CDCl_3$) δ 10.12, 14.37, 14.39, 19.0, 19.6, 19.7, 28.9, 33.8, 40.5, 59.8, 59.9, 102.3, 102.6, 120.7, 122.2, 127.5, 129.1, 129.8, 131.6, 142.2, 142.6, 142.7, 159.7, 166.8, 167.2, 172.1; MS (EI) 528, 530. Anal. Calcd for $C_{26}H_{31}N_2O_5Br$: C, 58.76; H, 5.88; N, 5.27. Found: C, 58.79; H, 5.96; N, 5.31.

6.4. Pharmacophore computational modeling

Ligand structures were drawn and energy minimized (Powell method, 0.01 kcal/mol*A gradient termination, MMFF94s force field, MMFF94 charges, 1000 maximum iterations) using the Sybyl modeling program (Tripos, St. Louis, MO, USA). Construction of the overlaying pharmacophore was achieved by assembling the energy minimized structures and merging the collection of structures into the same field. This was followed by energy minimization, molecular dynamics, and an energy minimization simulation. Aggregates for molecular dynamics and minimization simulations were defined as Carbons 2,3,4,5 and 6 of the 1,4-dihydropyridine ring. All ligands were then energy minimized to allow for the lowest energy confirmation of each ligand.

Acknowledgment

The authors thank the NIH for grants GM42029, NS038444, and P20RR015583.

MDR1 data was generously provided by the National Institute of Mental Health's Psychoactive Drug Screening Program (NIMH PDSP), Contract # HHSN-271-2008-00025-C (NIMH PDSP). The NIMH PDSP is Directed by Bryan L. Roth MD, PhD at the University of North Carolina at Chapel Hill and Project Officer Jamie Driscoll at NIMH, Bethesda MD, USA.

Supplementary data

Supplementary data associated with this article can be found, in the online version, at http://dx.doi.org/10.1016/j.bmc.2012.09.022.

References and notes

1. Linton, K. J. *Physiology* **2007**, *22*, 122.
2. (a) Aller, S. G.; Yu, J.; Ward, A.; Weng, Y.; Chittaboina, S.; Zhuo, R.; Harrell, P. M.; Trinh, Y. T.; Zhang, Q.; Urbatsch, I. L.; Chang, G. *Science* **2009**, *323*, 1718; (b) Globisch, C.; Pajeva, I. K.; Wiese, M. *ChemMedChem* **2008**, *3*, 280.
3. Nobili, S.; Landini, I.; Giglioni, B.; Mini, E. *Curr. Drug Targets* **2006**, *7*, 861.
4. (a) For elegant studies with exciting potential as theranostic agents see: Namanja, H.A.; Emmert, D.; Davis, D.A.; Campos, C.; Miller, D.A.; Hrycyna, C.A.; Chmielewski, J. *J. Am. Chem. Soc.* ASAP **2011**, http://dx.doi.org/10.1021/ja206867t.; (b) Pires, M. M.; Emmert, D.; Hrycyna, C. A.; Chmielewski, J. *Mol. Pharmacol.* **2009**, *75*, 92; (c) Pires, M. M.; Hrycyna, C. A.; Chmielewski, J. *Biochemistry* **2006**, *45*, 11695.
5. (a) Robey, R. W.; Shukla, S.; Finley, E. M.; Oldham, R. K.; Barnett, D.; Ambudkar, S. V.; Fojo, T.; Bates, S. E. *Biochem. Pharmacol.* **2008**, *3*, 1302; (b) Clinicaltrials.gov, search P-gp, accessed January 20, 2012.
6. Zamponi, G. *Voltage-Gated Calcium Channels*; Landes Bioscience: New York, 2005.
7. Nogae, I.; Kohno, K.; Kikuchi, J.; Kuwano, M.; Akiyama, S.-I.; Kiue, A.; Suzuki, K.-I.; Yoshida, Y.; Cornwell, M.; Pastan, I.; Gottesman, M. *Biochem. Pharmacol.* **1989**, *38*, 519.
8. (a) Mehdipour, A. R.; Javindnia, K.; Hemmateenejad, B.; Amirghorfran, Z.; Miri, R. *Chem. Biol. Drug Des.* **2007**, *70*, 337; (b) Miri, R.; Mehdipour, A. *Bioorg. Med. Chem.* **2008**, *16*, 8329.
9. Shah, A.; Bariwal, J.; Molnár, J.; Kawase, M.; Motohashi, N. *Top. Heterocycl. Chem.* **2008**, *15*, 201.
10. (a) Zhou, X. F.; Shao, O.; Coburn, R. A.; Morris, M. E. *Pharm. Res.* **2005**, *22*, 1989; (b) Zhou, X. F.; Zhang, L.; Tseng, E.; Scott-Ramsay, E.; Schentag, J. J.; Coburn, R. A.; Morris, M. E. *Drug Metab. Dispos.* **2005**, *33*, 321.
11. Hoellt, V.; Kouba, M.; Dietel, M.; Vogt, G. *Biochem. Pharmacol.* **1992**, *43*, 2601.
12. Natale, N. R.; Quincy, D. A. *Synth. Commun.* **1983**, *13*, 817.
13. Schauer, C. K.; Anderson, O. P.; Natale, N. R.; Quincy, D. A. *Acta Crystallogr.* **1986**, *C42*, 884.
14. McKenna, J. I.; Schlicksupp, L.; Natale, N. R.; Willett, R. D.; Maryanoff, B. E.; Flaim, S. F. *J. Med. Chem.* **1988**, *31*, 473.
15. Natale, N. R.; Triggle, D. J.; Palmer, R. B.; Lefler, B. J.; Edwards, W. D. *J. Med. Chem.* **1990**, *33*, 2255.
16. Mirzaei, Y. R.; Simpson, B. M.; Triggle, D. J.; Natale, N. R. *J. Org. Chem.* **1992**, *57*, 6271.
17. Palmer, R. B.; Andro, T. M.; Natale, N. R.; Anderson, N. H. *Magn. Reson. Chem.* **1996**, *34*, 495.
18. Natale, N. R.; Rogers, M. E.; Staples, R. J.; Triggle, D. J.; Rutledge, A. *J. Med. Chem.* **1999**, *42*, 3087.
19. Zamponi, G.; Stotz, S. C.; Staples, R. J.; Rogers, T. A.; Nelson, J. K.; Hulubei, V.; Blumenfeld, A.; Natale, N. R. *J. Med. Chem.* **2003**, *46*, 87.
20. (a) Natale, N. R.; Niou, C.-S. *Tetrahedron Lett.* **1984**, 3943; (b) Natale, N. R.; McKenna, J. I.; Niou, C.-S.; Borth, M.; Hope, H. *J. Org. Chem.* **1985**, *50*, 5660; (c) Niou, C.-S.; Natale, N. R. *Heterocycles* **1986**, *24*, 401.
21. Natale, N. R.; Mirzaei, Y. R. *Org. Prep. Proced. Int.* **1993**, *25*, 515.
22. Tiberghien, F.; Loor, F. *Anticancer Drugs* **1996**, *7*, 568–578.
23. Hamilton, G.; Cosentini, E. P.; Teleky, B.; Koperna, T.; Zacheri, J.; Riegler, M.; Feil, W.; Schiessel, R.; Wenzi, E. *Anticancer Res.* **1993**, *13*, 2059.
24. Crivori, P.; Reinach, B.; Pezzetta, D.; Poggesi, I. *Mol. Pharm.* **2006**, *3*, 33.
25. Dawson, R. J. P.; Locher, K. P. *Nature* **2006**, *443*, 180.
26. (a) Ecker, G.; Huber, M.; Schmid, D.; Chiba, P. *Mol. Pharmacol.* **1999**, *56*, 791; (b) Ecker, G.F.; Schwaha, R.; Demel, M.; Chiba, P. Pharmacoinformatic approaches to target P-glycoprotein: from inhibitor design to substrate prediction. ACS 235th National Meeting, New Orleans, LA, April 6–10, 2008, Abstract MEDI 161.
27. Sirisha, K.; Shekhar, M. C.; Umasankar, K.; Mahendar, P.; Sadanandam, A.; Achaiah, G.; Reddy, V. M. *Bioorg. Med. Chem.* **2011**, *19*, 3249.